Control of Inverted Pendulum: A comparative study on sliding mode approaches

Farbood Shokouhi
School of Mechanical Engineering
Iran University of Science and Technology (IUST)
Tehran, Iran.
shokuhi@gmail.com, ORCID: 0000-0002-4627-8767

Amir Hossein Davaie-Markazi[1]
School of Mechanical Engineering
Iran University of Science and Technology (IUST)
Tehran, Iran.
markazi@iust.ac.ir, ORCID: 0000-0003-4077-2614

Abstract – An under-actuated mechanical system (UMS) has fewer control inputs than the number of degrees of freedom (DoF). Such systems are frequently encountered in a wide range of applications, including robotic and aerospace systems. Control of an under-actuated Single Inverted Pendulum (SIP) is a well-known benchmark problem for research purposes. Sliding mode controllers (SMCs) are frequently used as robust control schemes applicable to nonlinear systems. In this study, three different versions of the SMC method are applied to a SIP, and performance comparisons are made. Since SIP is under-actuated, a diffeomorphism, i.e., a smooth transformation with a smooth inverse, is first applied so that the system equations are mapped into a standard form for which SMC-based methods could be applied. In particular, it is shown that the so-called Power Rate Exponential Reaching (PRER) method has a better performance compared to the Constant Rate Reaching (CRR) and the Exponential Rate Reaching (ERR) approaches. Furthermore, a new smooth and approximate switch function is proposed and closed-loop stability is proved.

Keywords—Sliding Mode Control (SMC), Single Inverted Pendulum (SIP), Switching function, Constant Rate Reaching (CRR) law, Exponential Rate Reaching (ERR) law, Power Rate Exponential Reaching (PRER) law.

I. INTRODUCTION

Under-actuated Mechanical Systems (UMSs) are frequently encountered in the fields of robotics. They have fewer actuators than DoF. In these systems, it is found that manipulators, vehicles, and humanoids with several passive joints. UMC arises by deliberating in the design to reduce the weight of the manipulator or might be caused by actuator failures. The difficulty in controlling under-actuated mechanisms is due to the fact that techniques, developed for fully actuated systems, cannot be directly used. These systems are not feedback linearizable, yet they exhibit nonholonomic constraints and nonminimum phase characteristics [1]. A SIP system, for example, is one of these systems.

A SIP on a cart presents a classical problem in dynamics and control theory due to its complex, multivariable, nonlinear, and unstable system. It consists of two DoF and a SIP which is attached to a cart where the only actuated DoF provides the horizontal motion of the cart. This means that for all control algorithms to be tested on this system, the main objective is to stabilize the pendulum in the upright position for any given initial pendulum position above the horizontal axis [2].

One of the key points in the designing controllers is that control must be done in the presence of bounded external unknown disturbances as well as perturbation-parametric uncertainties. In recent years, for this purpose, there has been a lot of researches on systems that have such conditions. In these extensive studies, the authors of these researches have been able to develop robust control methods for such conditions, in which SMC based on Lyapunov designing is the most important of these methods. The SMC has been always considered an efficient approach in control systems, due to its high accuracy and robustness concerning various internal and external disturbances [3]. Utkin et al. were among the pioneer researchers to discuss the chattering Problem in SMC Systems [4]. Edwards et al. considered the application of a particular sliding mode observer to the problem of fault detection and isolation [5]. Qin et al. designed an optimal switching function for SMC and developed a high-order control design methodology for a rotary flexible joint having constant delay time and uncertain parameters with known upper and lower bounds [6]. Grossimon et al. considered a sliding mode controller for a rotational inverted pendulum [7].

One proposition of this paper is to employ a new Continuous Approximation of Sign Function (CASF) instead of the conventional sign function, to overcome the unwanted chattering phenomena in the system response. Three different approaches for switching functions are discussed and used in this work.

This paper has eight sections and the organization is as follows: In section I, there is stated a brief introduction to the work done by researchers on the SIP with the SMC approach. In Section II the SIP system is described. In section III, the SMC approaches are introduced. In Section IV, the switching procedure of the switching function is expressed. In Section V, the controller design methodology is presented. In section VI, numerical simulation is performed and the corresponding graphs are drawn. In Section VII, the numerical simulation results are discussed. In Section VIII, the necessary conclusion and discussion are summed up.

II. SINGLE INVERTED PENDULUM SYSTEM

Models can be used for simulations, analysis of the system's behavior, a better understanding of the underlying

[1] - Correspond author

mechanisms in the system, design of new processes, or design of controllers. Traditionally, modeling is seen as a conjunction of a thorough understanding of the system's nature and behavior, and of a suitable mathematical treatment that leads to a usable model [8].

The SIP system presented here consists of a pendulum, a cart, a straight-line rail, and a driving unit (Fig. 1). The cart can move right or left on the rail freely. The pendulum is hinged in the center of the top surface of the cart and can rotate around the pivot in the same vertical plane with the rail. System parameters are shown in Table I [9].

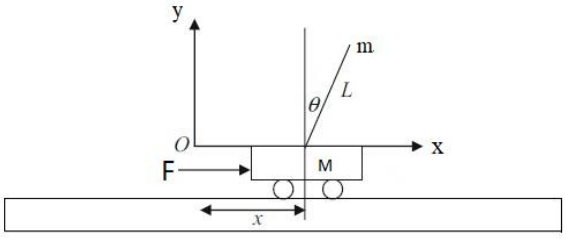

Fig. 1. Configuration of the SIP and car system

TABLE I. SYSTEM PARAMETERS

Description	*Notation*	*Subhead*
Mass of the pendulum	m	0.1 [kg]
Mass of the cart	M	1.0 [kg]
Length to pendulum center of mass	L	0.5 [m]
Gravitation acceleration	g	9.81 [$^{m}/_{s^2}$]
Pendulum's Moment of Inertia	J	4×10^{-7} [kg.m^2]
Pendulum angle from vertical	θ	- [Rad]
Angular velocity	$\dot{\theta}$	- [$^{Rad}/_{s}$]
Position of the cart from the rail origin	x	- [m]
Velocity of the cart from the rail origin	$\dot{x}$	- [$^{m}/_{s}$]
Viscous damping coefficient of pendulum axis	B_p	0.0026 [$^{N.s.m}/_{rad}$]
Equivalent coefficient of dry friction on cart surface	B_{eq}	5.7 [$^{N.s}/_{m}$]

III. DYNAMIC EQUATION OF SIP

The dynamical behavior of an inverted pendulum can be described by the following differential equations [10].

$$(M+m)\ddot{x} + (B_{eq}+K_2)\dot{x} - mL\ddot{\theta}Cos\theta + mL\dot{\theta}^2 Sin\theta = K_1 u \quad (1)$$

$$(J+mL^2)\ddot{\theta} + B_p\dot{\theta} - m\ddot{x}LCos\theta - mgLSin\theta = 0 \quad (2)$$

where K_1 and K_2 are factors that are satisfied in the following equation. Here the values of $K_1 = 1.7$ and $K_2 = 7.7$ are considered:

$$F = K_1 u - K_2 \dot{x} \quad (3)$$

Making $\ddot{\theta}$ the subject in (2) gives

$$\ddot{\theta} = \frac{m\ddot{x}LCos\theta + mgLSin\theta - B_p\dot{\theta}}{(J+mL^2)} \quad (4)$$

Making $\ddot{x}$ the subject in (2) gives

$$\ddot{x} = \frac{(J+mL^2)\ddot{\theta} + B_p\dot{\theta} - mglsin\theta}{mlcos\theta} \quad (5)$$

Putting (4) in (1) and making the subject yields equation (6) below

$$\ddot{x} = \frac{-(j+mL^2)B_{eq}\dot{x} - mLB_p\dot{\theta}Cos\theta - (JmL+m^2L^3)\dot{\theta}^2 Sin\theta + m^2L^2 gSin\theta Cos\theta - (J+mL^2)K_2\dot{x}}{m^2L^2(Sin\theta)^2 + MmL^2 + J(M+m)} + \frac{(J+mL^2)K_1}{m^2L^2(Sin\theta)^2 + MmL^2 + J(M+m)}u \quad (6)$$

Putting (5) in (2) and making the subject yields (7) below

$$\ddot{\theta} = \frac{-(M+m)B_p\dot{\theta} - m^2L^2\dot{\theta}^2 Sin\theta Cos\theta - mLB_{eq}\dot{x}Cos\theta + (m+M)mgLSin\theta - K_2mL\dot{x}Cos\theta}{m^2L^2(Sin\theta)^2 + MmL^2 + J(M+m)} + \frac{K_1mLCos\theta}{m^2L^2(Sin\theta)^2 + MmL^2 + J(M+m)}u \quad (7)$$

Equations (6) and (7) are therefore the differential equations for SIP with actuator dynamics.

A. State-space equation of SIP

To express the differential equation of the IP derived in the state space, the following state variables are defined for the system:

$$\begin{cases} x_1 = x \\ x_2 = \dot{x}_1 = \dot{x} \\ x_3 = \theta \\ x_4 = \dot{x}_3 = \dot{\theta} \end{cases} \quad (8)$$

For simplicity, the following parameters are considered:

$$\begin{cases} a_1 = (J + mL^2) \\ a_2 = JmL + m^2L^3 \\ a_3 = m^2L^2 g \\ a_4 = MmL^2 + J(M+m) \\ a_5 = (M+m)mgL \end{cases} \quad (9)$$

and also

$$\begin{cases} f_2 = \frac{-a_1B_{eq}x_2 - mLB_px_4Cosx_3 - a_2x_4{}^2Sinx_3 + a_3Sinx_3Cosx_3 - a_1K_2x_2}{m^2L^2(Sinx_3)^2 + a_4} \\ f_4 = \frac{-(M+m)B_px_4 - m^2L^2x_4{}^2Sinx_3Cosx_3 - mLB_{eq}x_2Cosx_3 + a_5Sinx_3 - K_2mLx_2Cosx_3}{m^2L^2(Sinx_3)^2 + a_4} \\ g_2 = \frac{a_1K_1}{m^2L^2(Sinx_3)^2 + a_4} \\ g_4 = \frac{K_1mLCosx_3}{m^2L^2(Sinx_3)^2 + a_4} \end{cases} \quad (10)$$

The state-space representation of SIP with actuator is therefore

$$\begin{cases} \dot{x} = F(X) + G(X)u \\ y = h(x) \\ h(x) = \begin{pmatrix} x_1 \\ x_3 \end{pmatrix} \\ x = \begin{pmatrix} x_1 \\ x_2 \\ x_3 \\ x_4 \end{pmatrix} \end{cases} \quad (11)$$

and

$$\begin{cases} F(X) = \begin{pmatrix} x_2 \\ f_2(x) \\ x_4 \\ f_4(x) \end{pmatrix} \\ G(X) = \begin{pmatrix} 0 \\ g_2(x) \\ 0 \\ g_4(x) \end{pmatrix} \end{cases} \quad (12)$$

B. Input-space linearization of SIP

By embedding (12) in (11)

$$\begin{pmatrix} \dot{x}_1 \\ \dot{x}_2 \\ \dot{x}_3 \\ \dot{x}_4 \end{pmatrix} = \begin{pmatrix} x_2 \\ f_2(x) \\ x_4 \\ f_4(x) \end{pmatrix} + \begin{pmatrix} 0 \\ g_2(x) \\ 0 \\ g_4(x) \end{pmatrix} u \quad (13)$$

[11], [12] proposed a method that can approximate the original system with an input-output linearizable control system in new coordinates. This stabilization method of a nonlinear system using sliding mode control is based on coordinate transformation by the mapping $T : x \rightarrow z$ defined by:

$$z_i = L_f^{i-1} h(x), \quad i \in 1,2,3,4 \quad (14)$$

with $z = (z_1 \quad z_2 \quad z_3 \quad z_4)^T$. T is defined as a local diffeomorphism with T(0) =0.

The dynamical system in the new coordinates can be approximated by the system model:

$$\begin{cases} \dot{z}_1 = z_2 \\ \dot{z}_2 = z_3 \\ \dot{z}_3 = z_4 \\ \dot{z}_4 = L_f^4(T^{-1}(z)) + L_g L_f^3 h(T^{-1}(z))u \end{cases} \quad (15)$$

$L_f h(x)$ is the Lie derivative of $h(x)$ along the vector $F(X)$. Consider the output system function of (11) defined by [12]:

$$h(x) = x_1 - L.\ln(\tan(x_3) + \sec(x_3)) \quad (16)$$

With the output $y = h(x)$ as obtained in (16), it is proceeded to find the diffeomorphism $z = T(x) = (y \quad \dot{y} \quad \ddot{y} \quad \dddot{y})^T$ as follows:

$$y = x_1 - L.\ln(\tan(x_3) + sec(x_3)) \quad (17)$$

$$\dot{y} = x_1 - \frac{Lx_4}{Cos(x_3)} \quad (18)$$

$$\ddot{y} = -\tan(x_3)\left(g + \frac{Lx_4^2}{Cos(x_3)}\right) \quad (19)$$

$$\dddot{y} = \left(\frac{-2}{(Cos(x_3))^2} + \frac{1}{Cos(x_3)}\right) Lx_4^3 + \left(\frac{-3g}{(Cos(x_3))^2} + 2g\right) x_4 - (2x_4 \tan(x_3))w \quad (20)$$

$$y^{(4)} = Lx_4^4 \left(\frac{-6Sin(x_3)}{(Cos(x_3))^2} + \frac{Sin(x_3)}{Cos(x_3)}\right) - \frac{6gx_4^2 Sin(x_3)}{Cos(x_3)^3} + 3x_4^2 \left(\frac{-2gSin(x_3)}{(Cos(x_3))^3} + \frac{gSin(x_3)}{Cos(x_3)}\right) + \frac{gSin(x_3)}{L}\left(\frac{-3g}{(Cos(x_3))^2} + 2g\right) + \left(\frac{-6x_4^2}{(Cos(x_3))^2} + 3x_4^2 - \frac{3g}{LCos(x_3)} + \frac{2gCos(x_3)}{L}\right) w = F_e(x) + G_e(x)w \quad (21)$$

The diffeomorphism T(x) is therefore defined as:

$$z = T(x) = \begin{pmatrix} h(x) \\ L_f h(x) \\ L_f^2 h(x) \\ L_f^3 h(x) \end{pmatrix} = \begin{pmatrix} z_1 = T_1(x) \\ z_2 = T_2(x) \\ z_3 = T_3(x) \\ z_4 = T_4(x) \end{pmatrix} \quad (22)$$

then

$$T(x) = \begin{pmatrix} y \\ \dot{y} \\ \ddot{y} \\ \dddot{y} \end{pmatrix} = \begin{pmatrix} x_1 - L.\ln(\tan(x_3) + sec(x_3)) \\ x_1 - \frac{Lx_4}{Cos(x_3)} \\ -\tan(x_3)\left(g + \frac{Lx_4^2}{Cos(x_3)}\right) \\ \left(\frac{-2}{(Cos(x_3))^2} + \frac{1}{Cos(x_3)}\right) Lx_4^3 + \left(\frac{-3g}{(Cos(x_3))^2} + 2g\right) x_4 - (2x_4 \tan(x_3))w \end{pmatrix} \quad (23)$$

The appearance of the input *w* in the diffeomorphism T(x), makes it impossible to do a full state linearization of the system using the obtained output $y = h(x)$. This is not surprising as the differential equation solved to obtain the output was noninvolutive. To do an approximate feedback linearization, the coefficient $(2x_4 \tan(x_3))w$ of the input *w* is ignored in the diffeomorphism as it is approximately zero when the system is close to the equilibrium point X_0. Wherever this approximation is valid, a suitable controller can be designed for w to stabilize the nonlinear system and drive the output to $y = z_1$ to 0. However, far from the equilibrium X_0, the approximation made to obtain the state transformations becomes invalid and the system losses the relative degree. This implies that the diffeomorphism obtained with the defined output is a local diffeomorphism. Defining the state variables for the approximately linearized system so that $z_1 = y = T_1(x)$, $z_2 = \dot{y} = T_2(x)$, $z_3 = \ddot{y} = T_3(x)$, $z_4 = \dddot{y} = T_4(x)$ and ignoring the coefficient of *w* in (20), the approximately linearized system is the one shown in (24):

$$\begin{cases} \dot{z}_1 = z_2 \\ \dot{z}_2 = z_3 \\ \dot{z}_3 = z_4 \\ \dot{z}_4 = F_e(X) + G_e(X)w \\ z = z_1 \end{cases} \quad (24)$$

where

$$F_e(X) = Lx_4^4\left(\frac{-6Sin(x_3)}{(Cos(x_3))^2} + \frac{Sin(x_3)}{Cos(x_3)}\right) - \frac{6gx_4^2Sin(x_3)}{Cos(x_3)^3} + 3x_4^2\left(\frac{-2gSin(x_3)}{(Cos(x_3))^3} + \frac{gSin(x_3)}{Cos(x_3)}\right) + \frac{gSin(x_3)}{L}\left(\frac{-3g}{(Cos(x_3))^2} + 2g\right) \quad (25)$$

$$G_e(X) = \frac{-6x_4^2}{(Cos(x_3))^2} + 3x_4^2 - \frac{3g}{LCos(x_3)} + \frac{2gCos(x_3)}{L} \quad (26)$$

by neglecting $2x_4\tan(x_3)$ [12], a feedback linearizable nonlinear system in the state z is obtained, with:

$$\begin{cases} \dot{z}_1 = z_2 \\ \dot{z}_2 = z_3 \\ \dot{z}_3 = z_4 \\ \dot{z}_4 = F_e(z) + G_e(z)u \\ z = z_1 \end{cases} \quad (27)$$

Now a controller is then designed for the input using SMC to introduce robustness into the feedback linearized system [13].

IV. Design of Sliding Mode Control

The SMC creates a discontinuous control law and causes a limited switching around the desired switching function. Thus, the trajectory's motion of the state variables and the system dynamics must inevitably be oriented towards this switching function. On the other hand, the existence of such a control law creates an unwanted problem in the control of the sliding, i.e., the "chattering phenomena" occurs which ought to be reduced or eliminated in some ways. Various approaches have been suggested in the literature, mostly based on the continuous approximation of the discontinuous sign function. In [9] several types of these methods are presented.

SMC based on the theory of variable structure systems, has been widely applied to robust control of nonlinear systems. SMCs offer good stability, robustness, and consistent performance of a controlled system with uncertainties and external disturbances [15,26]. In general, the design of SMCs consists of two steps. The first is finding a feedback controller which causes the state trajectory to reach the sliding surface s in finite-time and thereafter remain on s. The second is to guarantee that the resulting trajectory on s is stable [24].

In summary, the advantages of this control method are as follows:

1 -It is not sensitive to changing model parameters.

2 -It is not sensitive to external disturbances and uncertainties.

3 -It has a quick response.

4 -There is no need for online recognition of the plant.

and the disadvantages of this control method are:

1 -Its main problem is creating a chattering phenomenon.

2- The control signal changes and switches between the two control structures. This creates a chattering phenomenon.

Consider the following nth order chaotic dynamical system

$$x^{(n)} = F(\boldsymbol{X}) + G(\boldsymbol{X})u \quad (28)$$

where $\boldsymbol{X} = [x \quad \dot{x} \quad \dots \quad x^{(n-1)}] = [x_1 \quad x_2 \quad \cdots \quad x_n] \in \mathbb{R}^n$ is the vector of states which are assumed to be measurable, $u \in \mathbb{R}$ is the control input, $F(\boldsymbol{X})$ and $G(\boldsymbol{X})$ are smooth functions that are not known a priori.

The tracking error is defined as

$$\boldsymbol{e}(t) = \boldsymbol{X}(t) - \boldsymbol{X}_d(t) = [e(t) \quad \dot{e}(t)]^T \quad (29)$$

The first time derivative of $\boldsymbol{e}(t)$ is:

$$\dot{\boldsymbol{e}}(t) = \dot{\boldsymbol{X}}(t) - \dot{\boldsymbol{X}}_d(t) \quad (30)$$

The objective is to determine a controller for the chaotic system described by (28), so that the tracking error converges to zero, i.e. $\lim_{n\to\infty} e(t) = 0$, while maintaining all signals bounded.

When the uncertainties occur, the system (28) is modified as

$$x^{(n)} = \left(F_n(\boldsymbol{X}) + \triangle F(\boldsymbol{X})\right) + \left(G_n(\boldsymbol{X}) + \triangle G(\boldsymbol{X})\right)u \quad (31)$$

in which F_n and G_n are the nominal values, and $\triangle F(\boldsymbol{X})$ and $\triangle G(\boldsymbol{X})$ are the uncertainties of F and G, respectively. Eq. (31) can be rewritten as

$$x^{(n)} = F(\boldsymbol{X}) + G(\boldsymbol{X})u + d \quad (32)$$

where d is the lumped uncertainty, defined as $d = \triangle F(\boldsymbol{X}) + \triangle G(\boldsymbol{X})$. It is assumed that the lumped uncertainty is bounded such that $|d| \le D$.

Let the time derivative operator be $D \triangleq d/dt$, and define a sliding surface as

$$s = F(\boldsymbol{X}) + G(\boldsymbol{X})u + d \quad (33)$$

High-accuracy and robustness against perturbation-parametric uncertainties and bounded external unknown disturbances. Therefore, SMC consists of a discontinuous control, in constraining the system states to reach in limited-time, and then to evolve into a switching function, a time-varying surface $s(t) \in \mathbb{R}^n$ is defined by equating the variable $s(\boldsymbol{X}(t), t)$, defined below, to zero.

$$s \doteq (D + \lambda)^{(n-1)}e(t), \quad 0 < \lambda, \ 0 \le t \quad (34)$$

and for n = 2 is:

$$s(t) \doteq \dot{e} + \lambda e \quad (35)$$

where, λ is a strictly positive constant which is taken to be the bandwidth of the system (the designer of the system chooses λ and differs throughout systems), $e(t) = x(t) - x_d(t)$ is the tracking error in the output state, $\dot{e}(t) = \dot{x}(t) - \dot{x}_d(t)$ is the tracking derivative error in the output state and $x_d(t)$ is the desired state.

It can be implied that λ is the slope of the line which is in quadrant II and IV of the phase plane $(e - \dot{e})$ (Fig. 2). Also, the tracking error vector is:

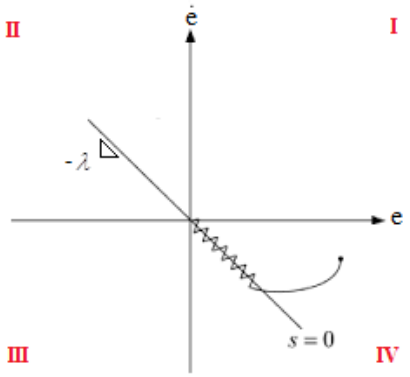

Fig. 2. Phase plane of $e(t) - \dot{e}(t)$

The problem of tracking the n-dimensional vector $\boldsymbol{X}_d(t)$ can be replaced by a first-order stabilization problem in s(t). $s(\boldsymbol{X}(t), t)$ verifying (30) is referred to as a switching function and the system's behavior once on the surface is called sliding mode or sliding regime. From (30) the expression of s(t) contains $\boldsymbol{e}^{(\boldsymbol{n-1})}(t)$, and it is only needed to differentiate s(t) once for the input u(t) to appear. Furthermore, bounds on s(t) can be directly translated into bounds on the tracking error vector $\boldsymbol{e}(t)$, and therefore the scalar s(t) represents a true measure of tracking performance [14].

The corresponding transformations of performance indices assuming $e(0) = 0$ is:

$$\forall\, 0 \le t, |s(t)| \le \phi \;\Rightarrow \forall\, 0 \le t, \left|e^{(i)}(t)\right| \le (2\lambda)^i \epsilon \qquad (36)$$

where $\epsilon = \frac{\phi}{\lambda^{(n-1)}}$ and $i = 1, \dots, n-1$. In this way, an nth-order tracking problem can be replaced by a first-order stabilization problem [15].

The simplified, first-order problem of keeping the scalar s(t) at zero can now be achieved by choosing the control law u(t) of (1) such that outside of s(t):

$$\frac{1}{2}.\frac{d}{dt}\left(s^2(t)\right) \le -\eta.|s(t)|, \quad 0 < \eta \qquad (37)$$

where η is a strictly positive constant. Condition (37) states that the squared "distance" to the surface, as measured by $s^2(t)$, decreases along all system trajectories. Thus, it constrains trajectories to point towards the surface s(t). In particular, once on the surface, the system trajectories remain on the surface. In other words, satisfying the sliding condition makes the surface an invariant set (a set for which any trajectory starting from an initial condition within the set remains in the set for all future and past times). Furthermore (37) also implies that some bounded external unknown disturbances or dynamic uncertainties can be tolerated while still keeping the surface an invariant set.

Finally, satisfying (34) guarantees that if $X(t = 0)$ is actually off $X_d(t = 0)$, the surface s(t) will be reached in a finite time smaller than $|s(t = 0)|/\eta$. Assume for instance that:

1) $0 < s(t = 0)$

2) Let t_{reach} be the time required to hit the surface $s = 0$. Integrating (37) between t=0 and $t = t_{\text{reach}}$ leads to:

$$0 - s(0) = s(t_{\text{reach}}) - s(0) \le -\eta.(t_{\text{reach}} - 0) \qquad (38)$$

which implies that

$$t_{reach} \le \frac{s(t=0)}{\eta} \qquad (39)$$

The similar result starting with $0 < s(t = 0)$ can be obtained as:

$$t_{\text{reach}} \le \frac{|\, s(t=0)\,|}{\eta} \qquad (40)$$

Starting from an initial condition, the state trajectory reaches the time-varying surface in a finite time smaller than $|\, s(t = 0)\,|/\eta$, and then slides along the surface towards $X_d(t)$ exponentially, with a time constant equal to $1/\lambda$.

To summarize, the idea is to use a well-behaved function of the tracking error s(t), according to (34), and then select u(t) such that $s(t)$ remains characteristic of a closed-loop system, despite the presence of model imprecision of disturbances.

A. *Conventional SMC (CSMC)*

CSMC contains a lot of notes and practical applications. The reason for this popularity is the attractive features of the sliding mode, which is simultaneously robust to "perturbation-model uncertainties" and "bounded external unknown disturbances". It also provides a "fast-convergence characteristic for a nonlinear system by following a reduced-order system" [14]. However, there are two problems in this method: The first problem is the "reaching phase" and the second one is the "input chattering problem" (chattering phenomena). In addition to these problems, the CSMC controller becomes much more conservative in its use than other design methods. Because the trajectories of motion are obtained by sliding mode dynamics, they cannot have dynamics as the main system [15]. In other words, the following factors cause the unwanted problem of "chattering phenomena":

1) Not being robust at the reaching phase.

2) Stimulate high-frequency unmodeled dynamics (with limited range) of a system; sensors or actuators.

3) Using the large gain in the controller.

4) Input control signal switching.

In addition to these problems, not guarantying asymptotic stability is also troublesome, which causes the system dynamics not to converge to a point of equilibrium in a limited time.

The design of a CSMC includes:

1) Determine a "switching function " that represents "desired stable dynamics", being robust at the reaching phase.

2) Describes a "control law" that guarantees "the reaching condition" and "the sliding condition".

The "phase trajectory" of a CSMC can be represented in two sections: the "reaching phase" (when the state trajectory is driven towards the switching function) and the "sliding phase" (when the state trajectory is moving towards the origin along the switching function), which will be reviewed in the following two modes of control (Fig. 3).

B. *Reaching phase*

In Fig. 3, the "reaching phase" of the desired starting point of the motion paths $x(t_0)$ to the switching function in a finite

time (i.e., point $x(t_1)$) was well demonstrated. The moving paths that start with a start condition given outside the switching function ($x(t_0)$) are dragged to the switching function ($x(t_1)$). This is known as the "reaching phase" or "hitting phase" ($\overline{x(t_0)x(t_{10})}$), and the system of CSMC is sensitive to "perturbation-model uncertainties" and "bounded external unknown disturbances" in this section of the "phase trajectory".

A designer must be able to reduce or eliminate this sensitivity in a variety of ways. The important point here is that if the initial error states are far from the switching function, the discontinuous control gain $(K(\boldsymbol{X}(t),t))$ will increase rapidly.

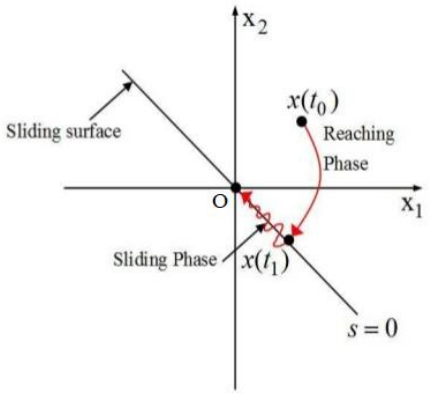

Fig. 3. The CSMC in phase plane [16]

This increase is due to the largeness of $|s(0)|$ and not due to perturbation-model uncertainties and bounded external unknown disturbances in the system. This is why the discontinuous control gain $(K(\boldsymbol{X}(t),t))$ is increased to an excessive amount. This incremental discontinuous control gain $(K(\boldsymbol{X}(t),t))$ causes error states to be forced on the switching function. That is why some researchers are talking about the elimination of the "reaching phase".

So far, various approaches have been proposed to eliminate the reaching phase:

1) Propose an integral sliding mode

2) Using the switching function of the time-varying (or switching function switching) [16]

3) Entering a larger control law [1]

4) Discontinuous control high-gain feedback to increase the speed of the reaching phase [1].

C. Sliding phase

According to Park et al. [17] states of the system, should be kept at the switching function. In other words, a "switching function" should be converted to an "absorbent surface" needed to design the "correct control law".

It is also one of the problems. Therefore, CSMC is very conservative in use with other controller design methods. This is why the state trajectory of the CSMC system is determined by sliding mode dynamics which cannot have the same order dynamics of the original system. An "absorbent switching function" is designed in the first stage and the controller which includes the determination of the "switching control law" is designed in the second stage. This law allows system states to stay on this surface after reaching it so that the system is balanced. To do this, the control law must be designed in such a way that the vectors of their state variables and their dynamics are tangent to the paths of movement to the surface [10].

Mendes has noticed that in practice, the Variable Structure Control (VSC) and especially SMC introduces a problem, and that is: there is only an "ideal sliding mode" when the state trajectory without any chattering moves toward the switching function and remains on it and proceeds to the equilibrium point. To solve this problem, Mendes suggests a continuous control law $u_{eq}(t)$ to be used that approaches the discontinuous law $u_{sw}(t)$ operation close to the switching surface region, thus obtaining a reference tracking with controlled accuracy [3].

There is a tradeoff relationship between "the level of chattering in the control signal" and "the accuracy in reference tracking". The more exact the tracking of references, the higher the level of chattering (Fig. 4).

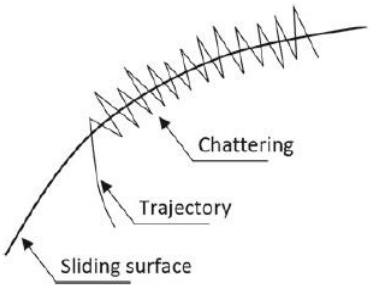

Fig. 4. A schematic of the level of chattering in the control signal around the switching function (or sliding surface) [18].

One of the recommendations based on eliminating unwanted chattering phenomena is substituting a Continuous Approximation of Sign Function (CASF) with the discontinuous sign function. So far, for this substitution, several functions have been proposed.

Our CASF proposal as follows [10]:

$$sign(s) \cong \frac{s}{\sqrt{s^2+\gamma}} \ , 0 < \gamma \tag{41}$$

The proposed function number (40) is an appropriate *CASF*. A designer can choose according to his design problem an appropriate value for the γ parameter. In this study, the value of $\gamma = 20$ is considered.

From (34), the time derivative of s can be obtained as

$$\dot{s} \doteq D(D+\lambda)^{(n-1)}e(t) = \left(D^n + \sum_{i=1}^{n-1} C^{n-1}D^{n-1}\lambda^i\right)e$$

$$= X^{(n)} - X_d^{(n)} + \sum_{i=1}^{n-1} C^{n-1}D^{n-1}\lambda^i \, e \tag{42}$$

where $C_r^n = (n!/(r!\,(n-r)!))$.

The control law consists of two parts: the first part is to reach the sliding surface (or reaching phase $u_{eq}(t)$) and the second step is sliding over the sliding surface (or sliding phase $u_{sw}(t)$).

$$u(t) = u_{eq}(t) + u_{sw}(t) \tag{43}$$

where $u(t) \in \mathbb{R}$ is the control law and the continuous control law $u_{eq}(t)$ is a feedback linearization controller, obtained from $\dot{s} = 0$ and (28) as

$$u_{eq}(t) = \frac{\left(-F(\boldsymbol{X}) + X_d^{(n)} - \sum_{i=1}^{n-1} C^{n-1} D^{n-1} \lambda^i e\right)}{G(\boldsymbol{X})} \quad (44)$$

and the discontinuous law $u_{sw}(t)$ is designed to dispel the uncertainties as

$$u_{sw}(t) = \frac{\delta sign(s)}{G(\boldsymbol{X})} \quad (45)$$

in which $sign(.)$ is the sign function. Substituting (43) – (45) into (32), and using (42) yields to

$$-d - \delta sign(s) = X^{(n)} - X_d^{(n)} + \sum_{i=1}^{n-1} C^{n-1} D^{n-1} \lambda^i e = \dot{s} \quad (46)$$

Then consider the following candidate Lyapunov function

$$V(s) = \frac{1}{2} s^2 \quad (47)$$

Differentiating (47) concerning time and using (46) yields to

$$\dot{V} = s\dot{s} = -sd - |s|\delta \leq |s||d| - |s|\delta = -|s|(\delta - |d|) \leq 0 \quad (48)$$

Therefore, the SMC system introduced in (43) can guarantee the stability of the uncertain system (32) in the Lyapunov sense.

In the design of the SMC, the uncertainty bound *d*, which includes unknown dynamics, parameter variations, and external load disturbance, must be available. However, the bound of uncertainties are difficult to obtain in advance for practical applications. Moreover, to satisfy the existing condition of the sliding mode, a conservative control law with large control effort usually results by using fixed, and most often conservative, bounds [24-25].

V. Design of Sliding Mode Controller for SIP

The controller design procedure consists of two steps: First step, a feedback control law u(t) is selected to verify sliding condition (37). However, in order to account for the presence of modeling imprecision of disturbances, the control law has to be discontinuous across s(t). Since the implementation of the associated control switching is imperfect, this leads to chattering, chattering is undesirable in practice since it involves high control activity and may excite high-frequency unmodeled dynamics neglected in the course of modeling. The first step achieves robustness for parametric uncertainty. The second step, the discontinuous control law $u_{sw}(t)$ is suitably smoothed to achieve an optimal trade-off between "control bandwidth" and "tracking precision". The second step achieves robustness to high-frequency unmodeled dynamics [14].

From (43) $u(t) \in \mathbb{R}$ is the control law and discontinuous sign function $sign(s)$ in $u_{sw}(t)$ that has covered the upper and lower part of the switching function. The control law u(t) with the discontinuous sign function $sign(s)$ creates a discontinuous control law $u_{sw}(t)$ that requires infinite switching around the switching function. In this way, the trajectory of the system states must be inclined toward the attractive switching function. On the other hand, due to the existence of such a control law, an unwanted problem in SMC, i.e., the "chattering phenomena" occurs which ought to be reduced or eliminated in some ways. The systems states being kept on the switching function is very crucial, but the existence of perturbation-model uncertainties and bounded external unknown disturbances causes the system states to be unable to stay put on the switching function, as a result, the "chattering phenomena" takes place [9].

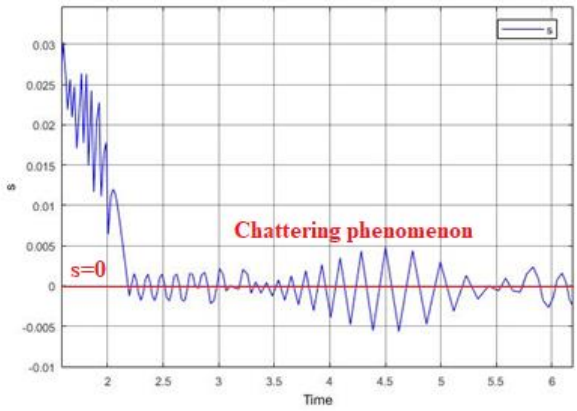

Fig. 5. A typical chattering phenomenon due to the switching effect of conventional SMCs.

In Fig. 5, the schematic available represents the “chattering phenomena" along with the "sliding phase".

So far, researchers have proposed different methods to solve the problem of unwanted chattering phenomena [10]. Since a discontinuous control law $u_{sw}(t)$ of the sliding phase depends on the definition of the switching function, each time using one of the three different approaches in $u_{sw}(t)$ to obtain a discontinuous control law $u_{sw}(t)$ on this basis. Below are three approaches, typically based on one of these approaches:

Approach 1: Constant rate reaching (CRR) law

Approach 2: Exponential Rate Reaching (ERR) law

Approach 3: Power Rate Exponential Reaching (PRER) law

Comment 1. There are many other reaching laws in the literature [19, 20, 21].

All these three approaches are implemented separately on a SIP.

Let $e = z - z_d$, $n = 4$ and the surface $s = \{z \in \mathbb{R}^4 | \, s(z) = 0\}$, for $0 < \lambda$.

$$s(z) = \left(\frac{d}{dt} + \lambda\right)^3 e \quad (49)$$

The time derivative of s along the system trajectory z is equal to:

$$\dot{s}(z) = z^{(4)} + 3\lambda z^{(3)} + 3\lambda^2 z^{(2)} + \lambda^3 z^{(1)} \quad (50)$$

$$\dot{s}(z) = f_e(z) + g_e(z)u + 3\lambda z^{(3)} + 3\lambda^2 z^{(2)} + \lambda^3 z^{(1)} = \Psi(z) + g_e(z)u \quad (51)$$

A. Approach 1

In (51), when $\dot{s}(z) = 0$, the best approximation of u is $\hat{u}$. $\hat{u}$ can be interpreted as our best estimate of the equivalent

control law $u_{eq}(t)$. To satisfy the sliding condition (37) despite uncertainty on the dynamics $f_e(z)$, the term "discontinuous ($u_{sw}(t)$)" across the surface $s(z) = 0$ is added to $\hat{u}$. Based on the sliding mode (43), the $u_{sw}(t)$ is a discontinuous control law. Constant Rate Reaching (CRR) law which has the form $u_{sw}(t) = -Q.sign(s).g_e(x), 0 < Q, g_e(x) < 0$ and drives the switching variable towards the switching surface at a constant rate, Q.

$$\begin{cases} u_{eq}(t) = -\frac{\Psi(z)}{g_e(z)} \\ u_{sw}(t) = -Qsign(s)g_e(x), 0 < Q, g_e(x) < 0 \end{cases} \quad (52)$$

The control action applied to the plant is therefore according to the transformations done in section III computed as in (53)

$$w = -\frac{\Psi(z)}{g_e(z)} + Q.sign(s).g_e(x) \quad (53)$$

$$u = \frac{w}{K_1}(m.sin^2x_3 + M) - \frac{mgsinx_3cosx_3 - mLx_4^2sinx_3 - (K_2+B_{eq})x_2}{K_1} \quad (54)$$

To demonstrate the stability with such a switching function, differentiating V along the trajectories of (47) and according to approach 1 is $\dot{s} = -Qsign(s), 0 < Q$ [13,15]. Also, using (41) to limit the chattering phenomena yields to

$$\dot{V} = s\dot{s} = s(-Qsign(s)) \cong s\left(-Q.\frac{s}{\sqrt{s^2+20}}\right) = -\frac{Qs^2}{\sqrt{s^2+20}} \leq 0 \quad (55)$$

Then the system is stable and the convergence of the sliding mode is guaranteed.

B. Approach 2

To continue, the Second-Order Sliding Mode Controller (SOSMC) is chosen to be used, because the drawback of the First-Order Sliding Mode Control (FOSMC) is the chattering phenomena. As a solution to resolve this problem, a Higher-Order Sliding Mode Control (HOSMC) algorithm is proposed. In fact, HOSMC appears as an effective application to counteract the chattering phenomena and the switching control signals, with higher relative degrees in limited-time [22]. The HOSMC has been introduced by Emel'yanov et al. [23], with the goal to get a finite time on the sliding set of order r defined by $s = \dot{s} = \ddot{s} = \cdots = s^{(r-1)} = 0$.

s defines the sliding variable with the rth-order sliding and with its $(r-1)$ first-time derivatives depending only on the state of x. The first order sliding mode tries to keep s = 0. In the case of Second-Order Sliding Mode Control (SOSMC), which only needs its measurement or evaluation of s, the following relation should be verified: $s(x) = \dot{s}(x) = 0$.

In (51), when $\dot{s}(z) = 0$, the best approximation of u is $\hat{u}$. $\hat{u}$ can be interpreted as our best estimate of the equivalent control law $u_{eq}(t)$. To satisfy the sliding condition (37) despite uncertainty on the dynamics $f_e(z)$, the term "discontinuous ($u_{sw}(t)$)" across the surface $s(z) = 0$ is added to $\hat{u}$. Based on the sliding mode (43), the $u_{sw}(t)$ is a discontinuous control law. Exponential Rate Reaching (ERR) law with the form $u_{sw}(t) = -(Ps + Q.sign(s)).g_e(x)$, $0 < P$, $0 < Q$, $g_e(x) < 0$ which drives the switching variable to the surface exponentially.

$$\begin{cases} u_{eq}(t) = -\frac{\Psi(z)}{g_e(z)} \\ u_{sw}(t) = -(Ps + Q.sign(s).g_e(x)) \end{cases} \quad (56)$$

The control action applied to the plant is therefore according to the transformations done in section III computed as in (57)

$$w = -\frac{\Psi(z)}{g_e(z)} + (Ps + Q.sign(s)).g_e(x) \quad (57)$$

$$u = \frac{w}{K_1}(m.sin^2x_3 + M) - \frac{mgsinx_3cosx_3 - mLx_4^2sinx_3 - (K_2+B_{eq})x_2}{K_1} \quad (58)$$

To demonstrate the stability with such a switching function, differentiating V along the trajectories of (47) and according to approach 2 is $\dot{s} = -(Ps + Qsign(s))$, $0 < P$, $0 < Q$ [13,15]. Also, using (41) to limit the chattering phenomena yields to

$$\dot{V} = s.\dot{s} = -s(Ps + Qsign(s)) \cong -s\left(Ps + Q.\frac{s}{\sqrt{s^2+20}}\right) = -Ps^2 - \frac{Qs^2}{\sqrt{s^2+20}} \leq 0 \quad (59)$$

Then the system is stable and the convergence of the sliding mode is guaranteed.

C. Approach 3

In (51), when $\dot{s}(z) = 0$, the best approximation of u is $\hat{u}$. $\hat{u}$ can be interpreted as our best estimate of the equivalent control law $u_{eq}(t)$. To satisfy the sliding condition (37) despite uncertainty on the dynamics $f_e(z)$, the term "discontinuous ($u_{sw}(t)$)" across the surface $s(z) = 0$ is added to $\hat{u}$. Based on the sliding mode (43), the $u_{sw}(t)$ is a discontinuous control law. Power Rate Exponential Reaching (PRER) law having the form

$$u_{sw}(t) = -\beta|s|^{\alpha}sign(s).g_e(x), \quad 0 < \beta, \quad 0 < \alpha < 1, \quad g_e(x) < 0$$

and drives the switching variable very fast when far from the surface but slower when close to the surface thereby reducing chattering.

$$\begin{cases} u_{eq}(t) = -\frac{\Psi(z)}{g_e(z)} \\ u_{sw}(t) = -\beta|s|^{\alpha}sign(s).g_e(x) \end{cases} \quad (60)$$

The control action applied to the plant is therefore according to the transformations done in section III computed as in (61)

$$w = -\frac{\Psi(z)}{g_e(z)} + \beta|s|^{\alpha}sign(s).g_e(x) \quad (61)$$

$$u = \frac{w}{K_1}(m.sin^2x_3 + M) - \frac{mgsinx_3cosx_3 - mLx_4^2sinx_3 - (K_2+B_{eq})x_2}{K_1} \quad (62)$$

To demonstrate the stability with such a switching function, differentiating V along the trajectories of (47) and according to approach 3 is $\dot{s} = -\beta|s|^{\alpha}.sign(s), 0 < \alpha < 1$, $0 < \beta$ [13,15]. Also, using (41) to limit the chattering phenomena yields to

$$\dot{V} = s\dot{s} = -s\left(\beta|s|^{\alpha} sign(s)\right) \cong -s\left(\beta|s|^{\alpha}\frac{s}{\sqrt{s^2+20}}\right) = -\frac{\beta|s|^{\alpha}s^2}{\sqrt{s^2+20}} \leq 0 \quad (63)$$

Then the system is stable and the convergence of the sliding mode is guaranteed.

VI. Numerical Simulation

By using the MATLAB and the following data this numerical simulation was done and its results are as the following:

A. Approach 1

For the simulation results, the design parameters are chosen as follows: $\lambda = 2.5, Q = 3.2$.

The initial condition is $x_0 = [{}^{\pi}/_{6} \quad 0 \quad 0 \quad 0]^T$. Thus, by applying the conventional sliding mode control (CSMC) to the SIP, the results shown in Fig. 6 and Fig.7 are obtained.

In Fig. 6 the pendulum angle against time for SMC with approach 1 can be seen. It is shown in this figure, despite the tilt angle deviation (30 degrees) of the pendulum from the vertical direction, the controller managed to keep up the pendulum vertically in the first few seconds. Also, it shows that position cart against time for SMC with approach 1. It is shown here that in the first few seconds, the controller managed to force the cart to keep the pendulum at its vertical line.

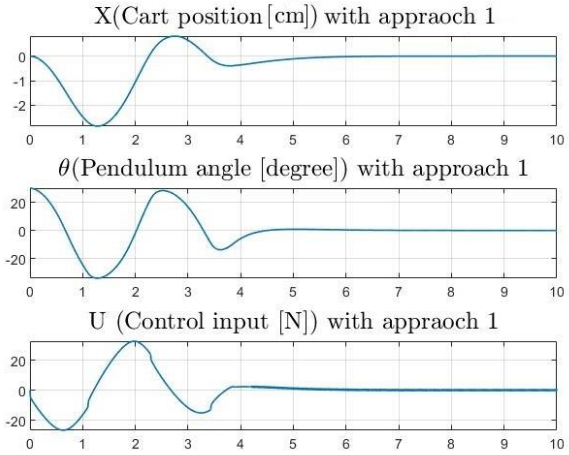

Fig. 6. Pendulum angle, cart position, and control law for SMC with approach 1

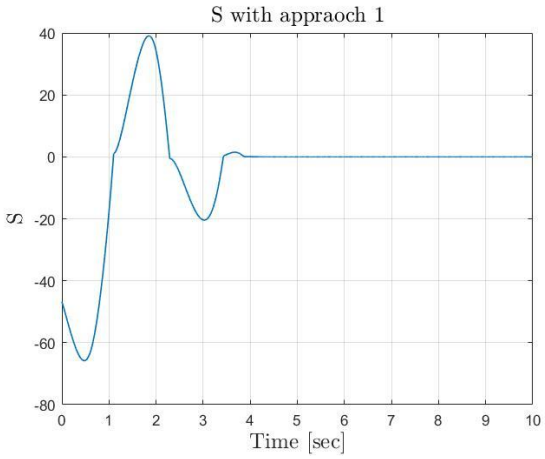

Fig. 7. Switching function (s) vs Time for SMC with approach 1

In Fig.7 in the first few seconds, our switching function converges to zero.

B. Approach 2

For the simulation results, the design parameters are chosen as follows: $\lambda = 2.5, Q = 2, P = 0.1$

The initial condition is $x_0 = [{}^{\pi}/_{6} \quad 0 \quad 0 \quad 0]^T$. Thus, by applying the conventional sliding mode control (CSMC) to the SIP, the results are shown in Fig. 8 and Fig. 9 are obtained.

In Fig. 8 the pendulum angle against time for SMC with approach 2 can be seen. It is shown in this figure, despite the tilt angle deviation (30 degrees) of the pendulum from the vertical direction, the controller can keep up the pendulum at its vertical line at a shorter amount of time than the approach 1. Also, it shows the position cart against time for SMC with approach 2. It is shown here that the controller with lesser force and lesser time to approach 1 can retain the pendulum in its vertical direction.

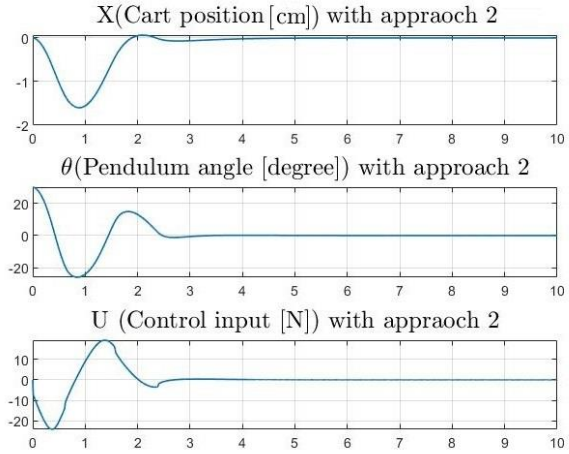

Fig. 8. Pendulum angle, cart position, and control law for SMC with approach 2

In Fig. 9 in the first few seconds, our switching function converges to zero. Also, the amplitude of switching function changes in approach 2 has been less than approach 1.

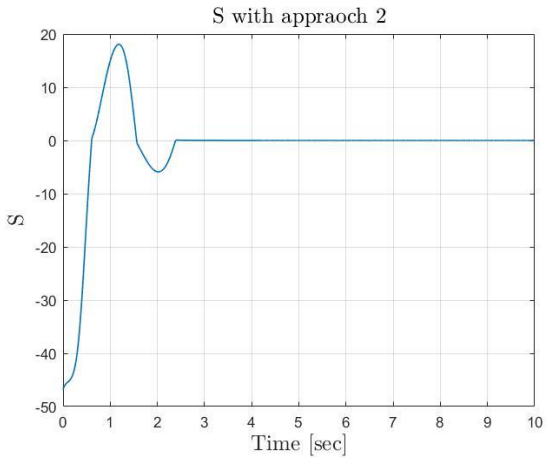

Fig. 9. Switching function (s) vs Time for SMC with approach 2

C. Approach 3

For the simulation results, the design parameters are chosen as follows: $= 2.5, \alpha = 0.4, \beta = 3$.

The initial condition is $x_0 = [\pi/6 \quad 0 \quad 0 \quad 0]^T$. Thus, by applying the conventional sliding mode control (CSMC) to the SIP, the results are shown in Fig. 10 and Fig. 11 are obtained.

In Fig. 10 the pendulum angle against time for SMC with approach 3 can be seen. It is shown in this figure, despite the tilt angle deviation (30 degrees) of the pendulum from the vertical direction, at a much shorter amount of time than the previous two approaches, the controller managed to reverse the pendulum to its vertical direction.

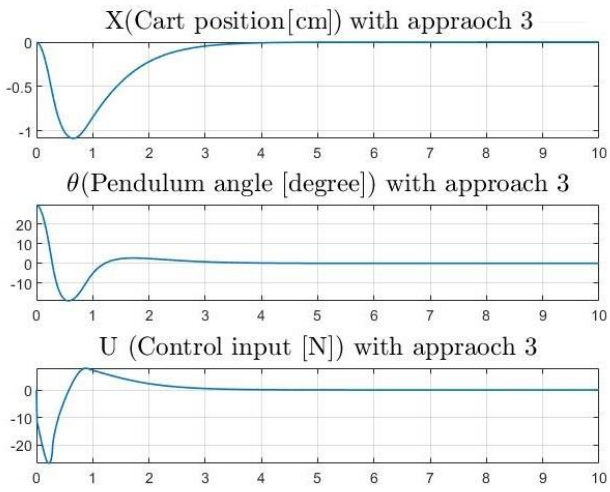

Fig. 10. Pendulum angle, cart position, and control law for SMC with approach 3

In Fig. 11 in the first few seconds, our switching function converges to zero. Also, the switching function converges to zero at a much shorter amount of time than the previous two approaches.

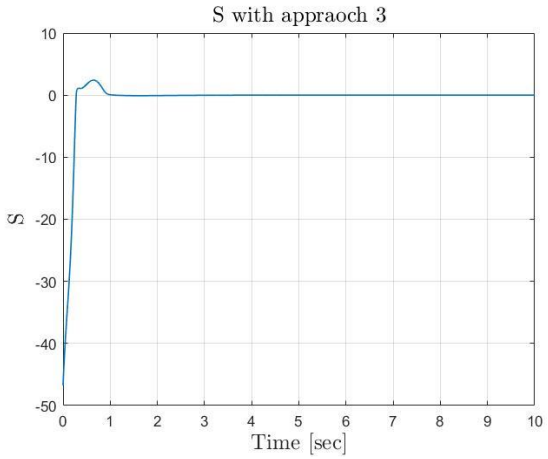

Fig. 11. Switching function (s) vs Time for SMC with approach 3

RESULTS AND DISCUSSION

In the following, the three different approaches are compared separately in terms of Cart position, Pendulum angle, Control input and then provide the performance indices for each of the three approaches in Tables II~VI (Fig. 12~14), respectively.

D. The results of the three approaches for the Cart position

Since the reduction of the overshoot value of the system leads to an increase in the stability, speed of the system, and improving the transient response, the smallest overshoot value in Table II (approach 3) is chosen. These are illustrated in Fig. 12.

$$Oversh.(X)_{.App.3} < Oversh.(X)_{.App.2} < Oversh.(X)_{.App.1}$$

TABLE II. OVERSHOOTS OF X

Overshoot			
	Approach 1	***Approach 2***	***Approach 3***
X	0.7	0.1	0

Based on Table III, the settling time value in approach 3 is smaller than the other settling time values. Thus approach 3 performs more efficiently than the other approaches. These are illustrated in Fig. 12.

$$Sett.time(X)_{.App.3} < Sett.time(X)_{.App.2} < Sett.time(X)_{.App.1}$$

TABLE III. SETTLING TIMES OF X [CM]

Settling time			
	Approach 1	***Approach 2***	***Approach 3***
X	6.1	4.3	3.8

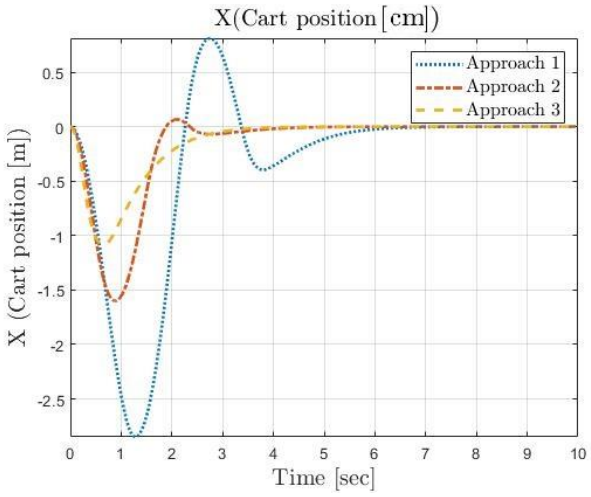

Fig. 12. The results of the three approaches for the Cart position

E. The results of the three approaches for the Pendulum angle

Since the reduction of overshoot systems leads to an increase in the stability, speed of the system, and improving the transient response, the overshoot value in systems needs to be reduced. Based on Table IV, the overshoot value of approach 3 is smaller than the overshoot values in approaches 1 & 2. These values are illustrated in Fig. 13.

$$Oversh.(\theta)_{.App.3} < Oversh.(\theta)_{.App.2} < Oversh.(\theta)_{.App.1}$$

TABLE IV. OVERSHOOTS OF θ

Overshoot			
	Approach 1	***Approach 2***	***Approach 3***
θ	28	10.2	0.2

Based on Table V, the lesser the settling time the more efficient the performance of the system. In Fig. 13 it can be seen that approach three is more optimum than the other two approaches.

$$Sett.time(\theta)._{App.3} < Sett.time(\theta)._{App.2} < Sett.time(\theta)._{App.1}$$

TABLE V. SETTLING TIMES OF θ

Settling time			
	Approach 1	***Approach 2***	***Approach 3***
θ	6.4	2.9	2.8

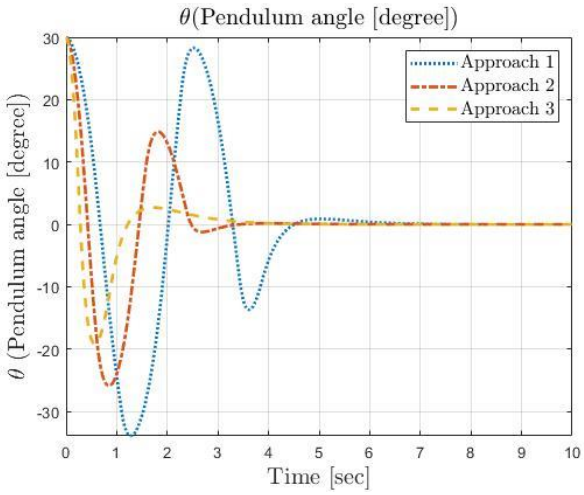

Fig. 13. The results of the three approaches for the Pendulum angle

F. *The results of the three approaches for the Control input*

The overshoot value in approach 3 is smaller than the overshoot value in the other approaches (Table VI). So, approach 3 was chosen. Here there is the need to choose the smallest overshoot value because the reduction of overshoot systems leads to an increase in the stability and speed of the system and also in improving the transient response, the overshoot value in the system is needed to be reduced. These are illustrated in Fig. 14.

$$Oversh.(u)._{App.3} < Oversh.(u)._{App.2} < Oversh.(u)._{App.1}$$

TABLE VI. OVERSHOOTS OF U

Overshoot			
	Approach 1	***Approach 2***	***Approach 3***
u	32	20.2	10

In Table VII, the settling time values in approach 2 & 3 are equal and they are smaller than the settling time value of approach 1. Thus, approaches 2 & 3 work more efficiently than approach 1. In Fig. 14, these points are illustrated.

$$Sett.time(u)._{App.3} = Sett.time(u)._{App.2} < Sett.time(u)._{App.1}$$

TABLE VII. SETTLING TIMES OF U

Settling time			
	Approach 1	***Approach 2***	***Approach 3***
u	5.7	2.7	2.7

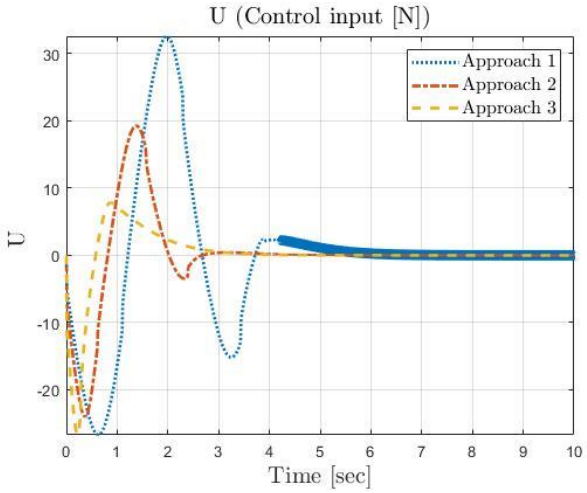

Fig. 14. The results of the three approaches for the Control input

In the control system theory, a performance index is a quantitative measure of the performance of a system and is chosen so that emphasis is given to the important system parameters. The performance of SMC with four indices (ISE= The Integral of the Square of the Error performance index, ISU= An index denoted as ISU can be used as a measure of how much the control action changes, J= A cost function that comes from the accumulation of ISE (Cart), ISE (Pendulum), and ISU indices) is compared to stabilized cart position of a SIP along with pendulum angle for an upright position. The parameters for the aforementioned control techniques are given in Table VIII.

$$ISE\ (Cart) = \int_{t_0}^{t_f} {X_1}^2(t)\,dt \tag{64}$$

$$ISE\ (Pendulum) = \int_{t_0}^{t_f} {X_3}^2(t)\,dt \tag{65}$$

$$ISU = \int_{t_0}^{t_f} u^2(t)\,dt \tag{66}$$

$$J = ISE\ (Cart) + ISE\ (Pendulum) + ISU \tag{67}$$

TABLE VIII. PERFORMANCE ANALYSIS OF THE CONTROL ALGORITHM

Control Algorithm / ***Performance***	***SMC Approach 1***	***SMC Approach 2***	***SMC Approach 3***
ISE (Cart)	202.3138	194.00	97.4615
ISE (Pendulum)	51.7409	20.3141	8.4995
ISU	128790.0838	41906.3869	20452.5492

Performance \ Control Algorithm	SMC Approach 1	SMC Approach 2	SMC Approach 3
J	129644.1385	42121.701	20558.5101

The performance indices for the three approaches are shown in Table VIII:

$$Perform._{App.1} < Perform._{App.2} < Perform._{App.3}$$

VII. CONCLUSION

In this paper, the Sliding Mode Control (SMC) performance was investigated with three different switching functions and the results were implemented on an inverted pendulum. Stability was proved for the three schemes.

By comparing three well-known approaches, i.e., the so-called Constant Rate, Exponential Rate, and Power Exponential Rate Reaching methods, it was revealed and concluded that the latter approach has a considerably better performance compared to the other studied methods.

REFERENCES

[1] Mendes, M. F., W. Kraus Jr, and E. R. De Pieri, "Variable structure position control of an industrial robotic manipulator", J. Brazilian Soc. Mech. Sci., vol. 24, no. 3, pp: 169–176, 2002.

[2] Roose, Ahmad Ilyas, Samer Yahya, and Hussain Al-Rizzo. "Fuzzy-logic control of an inverted pendulum on a cart." Computers & Electrical Engineering 61. pp: 31-47. 2017.

[3] A.Isidori. “Nonlinear Control Systems”, Springer Verlag, 1995.

[4] Utkin, Vadim, and Hoon Lee. "Chattering problem in sliding mode control systems." In Variable Structure Systems, 2006. VSS'06. International Workshop on, pp. 346-350. IEEE, 2006.

[5] Edwards, Christopher, Sarah K. Spurgeon, and Ron J. Patton. "Sliding mode observers for fault detection and isolation." Automatica 36, no. 4, pp: 541-553. 2000.

[6] Grossimon, Paul G., Enrique Barbieri, and Sergey Drakunov. "Sliding mode control of an inverted pendulum." In System Theory, Proceedings of the Twenty-Eighth Southeastern Symposium on, pp: 248-252. IEEE, 1996.

[7] Qin Z-C, Zhong S and Sun J-Q. "Sliding mode control experiments of uncertain dynamical systems with time delay." Communications in Nonlinear Science and Numerical Simulation 18. pp:3558–3566. 2013.

[8] Babuška, Robert. Fuzzy systems, modeling, and identification. Technical Report, 1997.

[9] Shokouhi, Farbood, and Davaie Markazi, Amir-Hossein. "A new continuous approximation of sign function for sliding mode control", International Conference on Robotics and Mechatronics (ICRoM 2018). Tehran. Iran. 2018.

[10] Chen, Chaio-Shiung, and Wen-Liang Chen. "Robust adaptive sliding-mode control using fuzzy modeling for an inverted-pendulum system." IEEE Transactions on Industrial Electronics 45, no. 2. pp: 297-306. 1998.

[11] Voytsekhovsky, Dmitry, and Ronald M. Hirschorn. "Stabilization of single‐input nonlinear systems using higher-order term compensating sliding mode control." International Journal of Robust and Nonlinear Control: IFAC‐Affiliated Journal 18, no. 4‐5. pp: 468-480. 2008.

[12] Aguilar, C., and R. Hirschorn. "Stabilization of an inverted pendulum." Report on Summer NSERC Research Project. 2002.

[13] Mahjoub, Sonia, Faiçal Mnif, and Nabil Derbel. "Second-Order Sliding Mode Control applied to an inverted pendulum." In 14th International Conference on Sciences and Techniques of Automatic Control & Computer Engineering-STA'2013, pp. 269-273. IEEE, 2013.

[14] Ming, Qian. "Sliding mode controller design for ABS system." Ph.D. diss., Virginia Tech, 1997.

[15] Slotine, J. and Li, W. "Applied Nonlinear Control". Prentice-Hall, New Jersey. 1991.

[16] E. K. S. In, "New Approaches for Online Tuning of the Linear Switching function Slope in Sliding Mode Controllers", vol. 11, no. 1, pp. 45–59, 2003.

[17] S. K. Park, S. K., and Ahn, H. K. "Robust controller design with novel sliding function", IEE Proceedings-Control Theory Appl., vol. 146, no. 3, pp. 242–246, 1999.

[18] Jedda, Olfa, Jalel Ghabi, and Ali Douik. "Sliding Mode Control of an Inverted Pendulum". In Applications of Sliding Mode Control, pp. 105-118. Springer, Singapore, 2017.

[19] C. J. Fallaha, M. Saad, H. Y. Kanaan, and K. Al-Haddad, "Sliding-mode robot control with exponential reaching law", IEEE Transactions on Industrial Electronics, vol. 58, no. 2, pp.600–610, 2011.

[20] M. Asad, A. I. Bhatti, and S. Iqbal, "A novel reaching law for smooth sliding mode control using the inverse hyperbolic function". in Proceedings of the International Conference on Emerging Technologies (ICET’ 12), pp. 1–6, Islamabad, Pakistan, October 2012.

[21] A.Wang, X. Jia, and S. Dong, “A new exponential reaching law of sliding mode control to improve performance of permanent magnet synchronous motor,” IEEE Transactions on Magnetics, vol. 49, no. 5, pp: 2409–2412, 2013.

[22] Bartolini, Giorgio, Arie Levant, A. Pisano, and E. Usai. "2-sliding mode with adaptation." In Proc. of the 7th IEEE Mediterranean Conference on Control and Systems. 1999.

[23] Emelyanov, S. V. "High-Order Sliding Modes in control systems." Differential equations 29 pp: 1627-1647. 1993.

[24] Poursamad, Amir, and Amir H. Davaie-Markazi. "Robust adaptive fuzzy control of unknown chaotic systems." Applied Soft Computing 9, no. 3, pp: 970-976. 2009.

[25] Lin, Chih-Min, and C-F. Hsu. "Self-learning fuzzy sliding-mode control for antilock braking systems." IEEE Transactions on Control Systems Technology 11, no. 2, pp: 273-278. 2003.

[26] H. Khalil, Nonlinear Systems, second ed., Prentice-Hall, New Jersey, 1996.